Biochemical Pharmacology 83 (2012) 1340–1348

Contents lists available at SciVerse ScienceDirect

Biochemical Pharmacology

journal homepage: www.elsevier.com/locate/biochempharm

Inhibition of the PI3K-Akt signaling pathway disrupts ABCG2-rich extracellular vesicles and overcomes multidrug resistance in breast cancer cells

Vicky Goler-Baron, Irina Sladkevich, Yehuda G. Assaraf *

The Fred Wyszkowski Cancer Research Laboratory, Department of Biology, Technion-Israel Institute of Technology, Haifa 32000, Israel

ARTICLE INFO

Article history:
Received 25 December 2011
Accepted 31 January 2012
Available online 8 February 2012

Keywords:
Extracellular vesicles (EVs)
PI3K-Akt signaling
Chemotherapy
ABC transporters
Overcoming multidrug resistance (MDR)
Breast cancer

ABSTRACT

We have recently shown that ABCG2-rich extracellular vesicles (EVs) form between neighbor breast cancer cells and actively concentrate various chemotherapeutics, resulting in multidrug resistance (MDR). Here we studied the signaling pathway regulating ABCG2 targeting to EVs as its inhibition would overcome MDR. The PI3K-Akt signaling pathway was possibly implicated in subcellular localization of ABCG2; we accordingly show here that pharmacological inhibition of Akt signaling results in gradual re-localization of ABCG2 from the EVs membrane to the cytoplasm. Cytoskeletal markers including β-actin and the tight junction protein ZO-1, along with the EVs markers ABCG2 and Ezrin–Radixin–Moesin revealed that this intracellular ABCG2 retention leads to gradual decrease in the size and number of EVs, resulting in EVs elimination and complete reversal of MDR. Inhibition of Akt signaling restored drug sensitivity to mitoxantrone and topotecan, *bona fide* ABCG2 transport substrates, hence being equivalent to MDR reversal achieved with the ABCG2 transport inhibitor Ko143. Remarkably, apart from loss of ABCG2 transport activity, treatment of MCF-7/MR cells with Ko143 resulted in cytoplasmic re-localization of ABCG2, similarly to the phenotype observed after Akt inhibition. We conclude that the PI3K-Akt signaling pathway is a key regulator of subcellular localization of ABCG2, EVs biogenesis and functional MDR. Furthermore, proper folding of ABCG2 and its targeting to the EVs membrane are crucial components of the biogenesis of EVs and their MDR function. We propose that Akt signaling inhibitors which disrupt ABCG2 targeting and EVs biogenesis may readily overcome MDR thus warranting *in vivo* studies with these promising drug combinations.

© 2012 Elsevier Inc. All rights reserved.

1. Introduction

The phosphatidyl-inositol 3-kinase (PI3K)-Akt signaling pathway integrates a plethora of extracellular signals to generate diverse physiological outcomes including cell proliferation, motility, glucose homeostasis, survival and cell death. Activation of the PI3K-Akt pathway is thought to play a pivotal role in both the initiation and progression of human breast cancer [1–3]. There are three principal components of the Akt pathway: PI3K, its antagonist PTEN and the serine/threonine kinase Akt, which is expressed as three structurally similar isoforms that differ in their expression pattern and function (recently reviewed in [1–3]). Receptor-mediated activation of the PI3K-Akt pathway occurs through Akt phosphorylation at threonine 308 and serine 473; upon activation, Akt translocates to the cytoplasm and the nucleus where it phosphorylates a variety of downstream targets. Two established isoform-unselective PI3K inhibitors are the fungal furanosteroid metabolite wortmannin which covalently binds to the conserved lysine 802 involved in the phosphate-binding reaction as well as LY294002, a reversible ATP-competitive PI3K inhibitor [2,4].

The frequent emergence of multidrug resistance (MDR) to structurally and functionally unrelated anticancer drugs is a major impediment to curative cancer chemotherapy [5–10]. ATP-driven MDR efflux transporters belong to the large ATP-binding cassette (ABC) superfamily of transporters that include ABCB1 (P-gp), ABCC1 (MRP1) and ABCG2 (BCRP). Overexpression of these efflux pumps results in the expulsion of a multitude of chemotherapeutic drugs, thereby leading to acquisition of a broad spectrum drug resistance known as MDR. We have recently identified [11] and characterized [12] a novel modality of MDR where neighbor breast cancer cells form extracellular vesicles (EVs) which overexpress ABCG2. These mitoxantrone (MR) resistant MCF-7/MR cells overexpress ABCG2 relatively to their parental cells and target ABCG2 specifically to the membrane of EVs where it mediates MDR. ABCG2-dependent sequestration of various cytotoxic agents including mitoxantrone [11], topotecan, methotrexate [12] and imidazoacridinones (unpublished data) within the lumen of EVs was abolished by the specific ABCG2 transport inhibitors Ko143 and fumitremorgin C (FTC) [13]. However, in spite of the important

* Corresponding author. Tel.: +972 4 8293744; fax: +972 4 8225153.
E-mail address: assaraf@tx.technion.ac.il (Y.G. Assaraf).

0006-2952/$ – see front matter © 2012 Elsevier Inc. All rights reserved.
doi:10.1016/j.bcp.2012.01.033

implications of these drug-concentrating EVs for cancer chemotherapy, nothing was known about the molecular mechanism by which ABCG2 is specifically targeted to the membrane of EVs. In this respect, recent studies suggested that the PI3K-Akt signaling pathway may regulate cellular localization of ABCG2. Moreover, Mogi et al. [14] and Bleau et al. [15] reported that exposure of *in vivo* isolated mouse hematopoietic stem cells known as side population (SP) as well as SP of glioma stem cells to the AKT inhibitor LY294002, resulted in translocation of ABCG2 from the plasma membrane to the cytoplasmic compartment. Consistently, Takada et al. [16], who examined ABCG2 localization in polarized porcine renal epithelial LLC-PK-1 cells that were stably transfected with the human ABCG2 found that Akt inhibition resulted in cytoplasmic internalization of ABCG2. However, when cells were incubated with epidermal growth factor, cell surface expression of ABCG2 increased. In contrast, Nakanishi et al. [17] reported that as opposed to the above studies, inhibition of the Akt signaling pathway in cultured chronic myelogenous leukemia cells induced down-regulation of ABCG2 expression rather than a shift in the sub-cellular localization of ABCG2 from the plasma membrane to the cytosol.

In the current study we explored the impact of the PI3K-Akt signaling pathway on ABCG2 protein expression and sub-cellular localization in the context of ABCG2-rich EVs formed in MR-resistant breast cancer (MCF-7/MR) cells [18]. We found that pharmacological inhibition of the PI3K-Akt signaling pathway results in a gradual retraction of ABCG2 from the EVs membrane to the cytoplasmic compartment, hence abolishing the ability of EVs to mediate anticancer drug sequestration. Simultaneously, we also detected a gradual disappearance of EVs, hence overcoming the MDR phenotype displayed by MCF-7/MR cells to the ABCG2 substrates MR and topotecan. Treatment of MCF-7/MR cells with the ABCG2-specific inhibitors Ko143 and FTC resulted not only in the expected abolishment of drug transport activity but also in cytoplasmic retention of ABCG2 and a time-dependent decrease in the number of EVs, similarly to the effect observed after PI3K-Akt signaling inhibition. In contrast, no effect of Akt signaling inhibition was found on ABCG2 protein levels. Taken altogether, these findings reveal that the PI3K-Akt signaling pathway is a key regulator of subcellular localization of ABCG2. We further conclude that ABCG2 is essential for the biogenesis of EVs and their MDR function.

2. Materials and methods

2.1. Chemicals

Mitoxantrone (MR), Ko143, FTC, epidermal growth factor (EGF) and 4′,6′-diamidino-2-phenylindole (DAPI) were purchased from Sigma–Aldrich (St. Louis, MO). Topotecan was a kind gift from Dr. K. Smid and Prof. G.J. Peters, VU University Medical Center, Amsterdam, The Netherlands. LY294002 was purchased from Promega Corporation, Madison, USA whereas Wortmannin was purchased from Alomone Labs, Israel.

2.2. Tissue culture

Human breast cancer MCF-7 cells and their MR-resistant subline MCF-7/MR cells [18], were grown as described previously [11,12]. Mycoplasma testing was routinely performed every 6 months using an established EZ-PCR Mycoplasma test kit (Biological Industries, Beth-Haemek, Israel). For live cell imaging experiments, cells were grown in custom-made riboflavin-deficient RPMI-1640 medium (Biological Industries, Beth-Haemek, Israel) supplemented with 10% dialyzed fetal calf serum (Invitrogen, Carlsbad, CA), glutamine and antibiotics.

2.3. Epidermal growth factor (EGF) stimulation

Exponentially growing MCF-7/MR cells were seeded onto 35 cm dishes ($\sim 2 \times 10^4$/2 ml; World Precision Instruments) and grown for 5 days to allow for optimal formation of EVs. Cells were then washed and incubated in serum-free medium for an additional 24 h. Next, cells were treated with LY294002 (20 μM) for 90 min, whereas controls were incubated in drug-free medium, all of which were followed with an EGF (50 ng/ml) stimulation for 5,10 and 30 min. Cells incubated in EGF-free medium served as the non-stimulated control ($t = 0$). Immediately following EGF stimulation, cells were harvested by placing culture dishes on ice-water and washed twice with ice-cold PBS. Cells were then lysed using lysis buffer (20 mM Hepes pH 7.4, 150 mM NaCl, 10% glycerol, 1% Triton X-100 and 1 mM EGTA; 1 mM $NaVO_4$ and protease inhibitors (Roche)), which were added immediately prior to use. Lysed cells were scraped off with a rubber policeman and placed on ice for an additional 30 min with vigorous vortexing from time to time. Then, lysates were centrifuged at 15,000 rpm at 4 °C for 20 min (Eppendorf Centrifuge 5417R) and the supernatants were collected. To assess Akt activity via its phosphorylation, equal amounts (20 μg protein/lane) of boiled cellular protein aliquots were resolved by electrophoresis on denaturing 10% polyacrylamide gels containing SDS and visualized using an antibody to phosphorylated-Akt (Ser473) (1:1000, Cell Signaling Technology, Boston, MA). Re-probing the blots with anti-Akt antibody (1:1000, Cell Signaling Technology, Boston, MA) served as a control.

2.4. Immunofluorescence microscopy

Cells were seeded on sterile glass coverslips in 24-well dishes (5×10^4 cells/2 ml) and grown for 7 days at 37 °C to allow for optimal formation of multiple EVs and immunofluorescence analysis was performed as previously described [12]. Specifically, ABCG2 was visualized using the monoclonal antibodies BXP-21 or BXP-53 (at 1:100 dilution, a generous gift of Dr. G.L. Scheffer and Prof. Rik Scheper), followed by incubation with FITC-conjugated donkey anti-mouse, or using rhodamine red-conjugated donkey anti-rabbit antibodies, respectively (1:100 dilution, Jackson ImmunoResearch Laboratories, West Grove, PA). The Ezrin–Radixin–Moesin (ERM) protein complex was visualized using rabbit monoclonal anti-ERM antibody (1:500 dilution, Epitomics, Burlingame, CA), which detects all three ERM proteins. ZO-1 was visualized with a mouse anti-ZO-1 monoclonal antibody (1:25 dilution, Invitrogen, Carlsbad, CA). Actin was followed using a rhodamine–phalloidin conjugate (Invitrogen, Carlsbad, CA). Cell nuclei were counterstained with the DNA dye DAPI (0.5 μg/ml). Cellular fluorescence was examined using either the Zeiss inverted Cell-Observer or the inverted confocal microscope (Zeiss LSM 700). Merged images were obtained using the AxioVision program (Zeiss, version 4.7).

2.5. Live cell imaging

Cells were seeded in culture dishes containing cover glass bottom (2×10^4 cells/2 ml; World Precision Instruments) and grown in riboflavin-free RPMI-1640 medium for 7 days to avoid the green autofluorescence of riboflavin [19]. Cells were then either pre-treated with LY294002 (20 μM) for 90 min or not, followed by an additional incubation with riboflavin (20 μM) for different time periods. Before analysis, cells were washed thrice with PBS and resuspended in PBS supplemented with 1 mM $CaCl_2$, 1 mM $MgCl_2$ and 10 mM D-glucose. Then, random colonies were analyzed using Zeiss inverted Cell-Observer microscope, equipped with a CO_2 containing chamber at 37 °C, using the following filters: phase

mode and HE GFP (excitation and emission at 470 ± 40 and 525 ± 50 nm, respectively).

2.6. Colorimetric cell proliferation assay

The cytotoxic activity of antitumor agents was determined using the XTT colorimetric cell proliferation kit (Biological Industries, Beth-Haemek, Israel), which measures metabolically active cells thus indirectly quantifies cell viability. Parental MCF-7 and MCF7/MR cells were seeded (400 cells/well) in 96-well plates and grown for 3 days to allow for the formation of EVs. Cells were then subjected for a 90 min pre-incubation with LY294002 (20 μM) or 1 h pre-incubation with Ko143 (0.7 μM), followed by co-incubation with increasing concentrations of MR or topotecan for additional 5 h or 72 h, respectively. In the case of MR cytotoxicity, viable cell numbers were determined after 72 h of treatment with MR. To determine the cytotoxic effect of LY294002 on MCF-7 and MCF-7/MR cells, cells were exposed to various concentrations of LY294002 for 6.5 h following 3 washes with fresh medium and incubated for additional 72 h prior to cell proliferation analysis. Drug concentrations required to inhibit cell growth by 50% (IC_{50}) were determined and compared between the cell lines.

2.7. Western blot analysis of ABCG2 levels

To examine the cellular expression levels of ABCG2 following LY294002 or Ko143 treatment, Western blot analysis was preformed with rat anti-ABCG2 antibody (BXP-53, at 1:1000 dilution, kindly provided by Dr. G.L. Scheffer) as described previously [20,21]. Likewise, an affinity-purified rabbit polyclonal antiserum to the α-subunit of Na^+/K^+ ATPase (anti-KETTY, at 1:3000 dilution, kindly provided by Prof. S.J. Karlish) and anti-actin antibody (Sigma, 1:10,000) were used as an indication of loading differences.

3. Results

3.1. Treatment of MCF-7/MR cells with LY294002 blocks Akt activation via inhibition of its phsophorylation

We postulated that the PI3K-Akt signaling pathway may regulate the differential sorting of ABCG2 to the membrane of EVs in MCF-7/MR cells. As a first step towards this end, we examined whether LY294002, an established Akt-effector protein inhibitor [2], could block the activation of the PI3K-Akt signaling pathway via inhibition of its phosphorylation. Thus, EVs-forming MCF-7/MR cells were stimulated with EGF for various times in the presence or absence of LY294002, following which phosphorylated-AKT (pAKT) protein levels were determined by Western blot analysis using a pAKT-specific antibody (Fig. 1A). After 5 min of stimulation with EGF, pAKT protein levels were already ~5-fold elevated as compared to non-stimulated cells. In contrast, when cells were pretreated for 90 min with LY294002 prior to EGF stimulation, AKT phosphorylation was markedly blocked (Fig. 1B). We calculated the extent of inhibition of AKT phosphorylation by dividing the values of pAKT levels following LY294002 treatment by the values obtained with untreated controls; after 5 min of LY294002 treatment, residual pAKT levels were 23%, whereas by the end of 30 min, only 15% of initial pAKT levels were detected. Thus, LY294002 achieved a marked inhibition of AKT phosphorylation.

Importantly, the 20 μM concentration of LY294002 was chosen based on multiple studies described in the literature that used this Akt signaling pathway inhibitor in different cell types including *in vivo* isolated mouse hematopoietic stem cells [14] as well as SP of glioma stem cells [15] and renal epithelial LLC-PK-1 cells [16]. Despite these ample data on the recommended LY294002 concentration, we examined the cellular effect of various concentrations of LY294002 on parental MCF-7 cells and their multidrug resistant MCF-7/MR subline. To this end, we exposed these breast cancer cell lines to different concentrations of LY294002 for 6.5 h; cells in monolayer were then washed three times with fresh growth medium and incubated for an additional 72 h prior to analysis. We found that the IC_{50} value for MCF-7 cells was above 300 μM and that IC_{50} value for MCF-7/MR cells was 210.8 ± 30 μM (Supplemental Fig. 1). Specifically, the fraction of viable MCF-7 cells treated with 20 μM LY294002 was 96.4 ± 3.9% and that of MCF-7/MR cells was 90.3 ± 6.7%. Based on these results we could not detect an off-target cytotoxic effect using 20 μM concentration of LY294002 in these breast cancer cell lines.

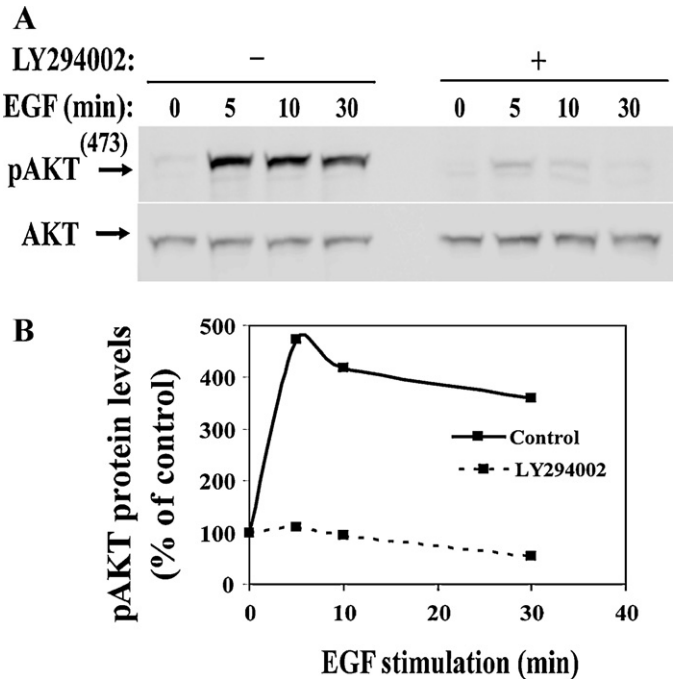

Fig. 1. Treatment of MCF-7/MR cells with LY294002 blocks AKT phosphorylation. (A) MCF-7/MR cells were seeded on 35 cm dishes (~2×10^4/2 ml) and grown for 5 days to allow for the formation of EVs. Then, cells were serum-starved for 24 h. Prior to stimulation with EGF, cells were either pre-incubated with or without LY294002 (20 μM) in serum-free medium for 90 min at 37 °C. Cells were then stimulated with EGF (50 ng/ml) at 37 °C for the indicated times. Immediately following stimulation, cells were harvested and lysed as detailed in Section 2. Equal amounts of total cellular protein (20 μg) were loaded for each sample, resolved on denaturing 10% polyacrylamide gels containing SDS and reacted with an anti-pAKT antibody (PhosphoSerine473). Total AKT protein levels were determined by stripping and re-probing of the blot with an anti-AKT antibody. (B) Graphic illustration of pAKT levels in LY294002-treated and untreated MCF-7/MR cells. Band intensity was quantified using an EZQuant-gel program, normalized to Akt and presented as percent pAKT level at time 0 in either treated or untreated cells.

3.2. Inhibition of the PI3K-Akt signaling pathway results in a time-dependent decrease in sorting of ABCG2 to EVs and consequent elimination of EVs

To address the question of whether or not the PI3K-Akt signaling pathway regulates subcellular localization of ABCG2, we used immunofluorescence microscopy and followed the subcellular localization of ABCG2 prior to and following Akt inhibition. Confocal microscopy revealed that after 90 min of treatment with LY294002, subcellular localization of ABCG2 was markedly altered. Consistent with our previous studies [12], ABCG2 was targeted

specifically to the EVs membrane (i.e. apical membrane) in control MCF-7/MR cells (Fig. 2A, (a and b)), whereas in LY294002-treated cells, ABCG2 was observed in the plasma membrane (i.e. basolateral membrane) and in the cytoplasm (Fig. 2A, (c–f), *dashed arrows*), in addition to its EVs localization (Fig. 2A, *continuous arrows*). Furthermore, LY294002 treatment for longer times revealed a time-dependent decrease in the size and number of EVs (Fig. 2A–C). In parallel, a gradually increasing ABCG2 fraction appeared in the cytoplasmic compartment and in the plasma membrane (Fig. 2B, g–l, *dashed arrows*) as well as at cell–cell attachment zones appearing as crucifer-like structures (Fig. 2B, g–l, *continuous arrows*). We previously identified these crucifer-like structures as premature EVs [12], hence disclosing the original site of formation of ball-like mature EVs. In all incubation times with LY294002, ABCG2 co-localized with ERM protein complex, an established structural marker of EVs [12] (Fig. 2B). In addition to confocal microscopy, the immunofluorescently-stained samples were analyzed using a Cell-Observer microscope, hence allowing for an enhanced detection of the cytoplasmic ABCG2 signal (data not shown); the obtained results were quantitatively validated and summarized in Fig. 2C. Consistent with the confocal microscopy results, we observed a gradual decrease in the size and number of EVs which was accompanied by a time-dependent increase in the cytoplasmic localization of ABCG2. Specifically, following 6 h of LY294002 treatment we observed a 30% decrease in the number of EVs compared to control cells, whereas the number of cells with cytoplasmic or plasma membrane localization of ABCG2 was increased by 61%. In contrast, Akt inhibition with LY294002 or wortmannin had no impact on ABCG2 protein levels (Fig. 2D).

To further examine the time-dependent elimination of EVs following LY294002 treatment, we performed a series of immunofluorescence studies with established cytoskeletal markers of EVs. ZO-1 is a tight junction (TJ) protein that localizes at the border between EVs-forming cells, in a belt-like pattern, hence sealing the

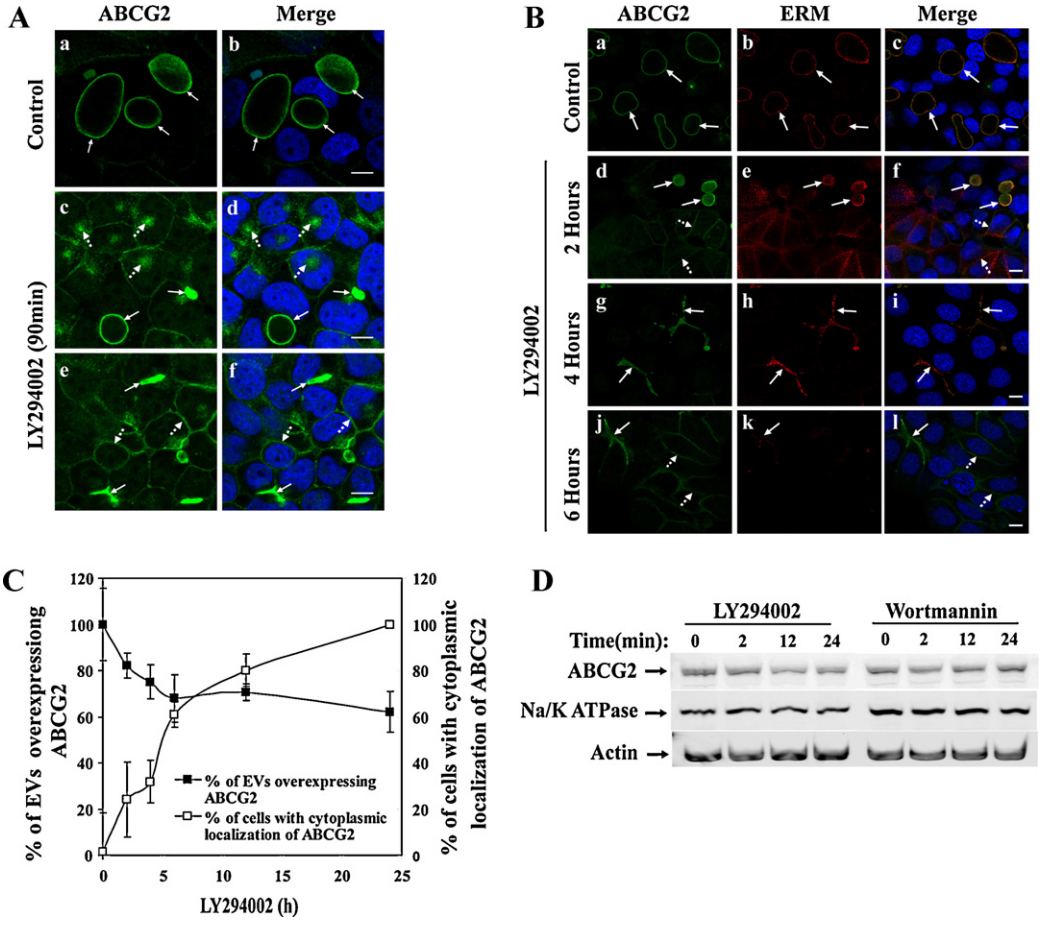

Fig. 2. The effect of LY294002 treatment on subcellular localization of ABCG2 and its protein levels in MCF-7/MR cells. (A) MCF-7/MR cells were grown in 24-well plates on sterile glass coverslips for 7 days at 37 °C to allow for optimal formation of EVs. Cells were then either untreated (a and b) or treated (c–f) with LY294002 (20 μM) for 90 min at 37 °C. Cells were then washed twice with PBS, fixed with 4% formaldehyde and co-reacted with anti-ABCG2 antibody (BXP-21) followed by incubation with secondary FITC-conjugated donkey anti-mouse antibody. Nuclei were counterstained with DAPI. Random colonies were analyzed using confocal LSM-700 laser microscope at a magnification of 630×. *Continuous arrows* point at EVs or cell–cell attachment zones, whereas *dashed arrows* denote cells with plasma membrane and cytoplasmic localization of ABCG2. (B) MCF-7/MR cells were grown as in (A) and treated with LY294002 for the indicated times. Then, cells were co-stained with both BXP-21 and with an anti-ERM antibody, which cross-recognizes all three ERM complex proteins. Random colonies were analyzed as in panel (A). Throughout the entire study the bar denotes10 μm. (C) A graphic illustration of ABCG2-rich EVs formation and ABCG2 localization following LY294002 treatment. MCF-7/MR cells were stained as described in (A) and photographed using the Zeiss inverted Cell-Observer microscope at a magnification of 630×. Then, random fields were analyzed for ABCG2-rich EVs or cells with cytoplasmic green signal of ABCG2. The number of EVs scored in untreated MCF-7/MR cells was defined as 100% and the numbers determined at the other time points were calculated relative to time 0 (presented by the left scale). ABCG2 appearing in cell–cell attachment zones was considered as EVs. The right scale presents the number of cells retaining ABCG2 in the plasma membrane and the cytoplasm and presented as the percentage of cells positively scored at time point 24 h. We defined cells with a cytoplasmic localization of ABCG2 when cells exhibited more green fluorescence in the cytoplasmic compartment than in untreated cells. To obtain these graphs, approximately 1000 cells were examined for each time point; results were plotted as a function of time. Graph represents three independent experiments for each time point, whereas error bars indicate standard deviation. (D) MCF-7 and MCF-7/MR cells were incubated with LY294002 or with wortmannin (200 nM)) for the indicated times. Then, membrane proteins were extracted and equal amounts of protein (60 μg) were loaded for each time point, resolved on denaturing 10% polyacrylamide gels and reacted with anti-ABCG2 antibody (BXP-53). Actual equal loading was verified using stripping and re-probing of the blot with an α-subunit Na^+/K^+ ATPase specific antibody (KETTY) or anti-actin antibody.

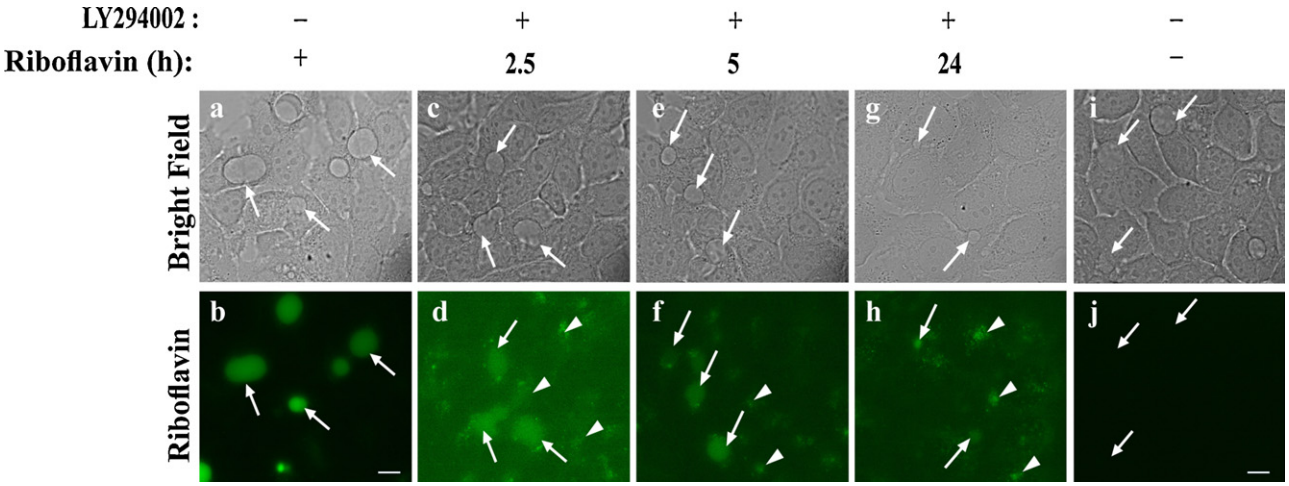

Fig. 3. LY294002-treated MCF-7/MR cells are unable to concentrate riboflavin in EVs. MCF-7/MR cells were seeded (1×10^4/6-well dish) in riboflavin-deficient medium for 7 days to allow for EVs formation. Then, cells were either pre-treated with LY294002 (20 μM) for 90 min or not (a and b), followed by an additional incubation with riboflavin (20 μM) for the indicated times (c–h). LY294002-untreated cells incubated in riboflavin-free medium served as control (i–j). At the end of the incubation period, cells were washed and examined using the Cell-Observer (630×) microscope using the same parameters. To minimize the background, the image in (j) was restored relatively to the positive control (b). Arrows denote the location of ABCG2-rich EVs; arrowheads denote the cytoplasmic location of riboflavin.

EVs to the outer environment and indicating the relative share that each cell contributes to the vesicular structure [12]. Co-staining of ZO-1 and ABCG2 revealed that EVs remained sealed to the outer environment by intact TJ structures following AKT-inhibition (Supplemental Fig. 2). Visualization of F-actin cytoskeleton, which normally reinforces EVs structures [12], revealed co-localization with the EVs marker ABCG2 prior to and following LY294002 treatment (Supplemental Fig. 3). However, this staining clearly underlines the gradual shrinkage in the volume of EVs with an intermediate step of ABCG2-rich crucifer-like structures and a gradual disruption of the EVs structures that occurs following LY294002 treatment.

3.3. Retraction of ABCG2 from the EVs membrane to sub-cellular compartments abolishes intravesicular accumulation of riboflavin

Our results show that treatment of ABCG2-rich EVs in MCF-7/MR cells with LY294002 results in a gradual re-localization of ABCG2 to the plasma membrane and the cytoplasmic compartment. We thus questioned whether inhibition of the PI3K-Akt signaling pathway abolishes the accumulation of ABCG2 transport substrates within EVs. To this end, MCF-7/MR cells were grown in riboflavin-deficient medium to avoid the intravesicular green fluorescence of riboflavin [19] and determined intravesicular accumulation of exogenous riboflavin (20 μM) prior to and following LY294002 treatment. Riboflavin was chosen as a representative non-cytotoxic ABCG2 chromophoric substrate that is effectively sequestrated within the lumen of EVs ([19]; Fig. 3a and b). Following a short treatment with LY294002 (90 min pre-incubation following co-incubation with riboflavin for additional 2.5 h), riboflavin fluorescence in EVs was markedly decreased (Fig 3c and d) and riboflavin was detected in cytoplasmic loci (*arrowheads*). Upon longer times of LY294002 treatment (5 h), the number of EVs markedly decreased and the fluorescence signal of riboflavin in EVs was much weaker than in control cells; moreover, riboflavin was now detected in cytoplasmic loci (Fig. 3e and f). Furthermore, following 24 h of treatment with LY294002, only rare EVs were detectable whereas predominant cytoplasmic riboflavin accumulation was apparent (Fig. 3g and h). Untreated cells incubated in riboflavin-free medium in the absence of exogenous riboflavin served as a control and showed no detectable green fluorescence (Fig. 3i and j). Under all treatments, cells were analyzed by a fluorescence microscope using the same parameters. These experiments established the differential localization of riboflavin following AKT inhibition, either in EVs or in cytoplasmic loci.

3.4. Inhibition of the PI3K-Akt signaling pathway by LY294002 overcomes MDR

Inhibition of the Akt-signaling axis results in a gradual retraction of ABCG2 from the EVs membrane into the cytoplasmic compartment, thus rendering EVs unable to concentrate riboflavin (Fig. 3). Based on these findings, we postulated that inhibition of the Akt-signaling pathway in MCF-7/MR cells may enhance the cytotoxic activity of antitumor agents which are ABCG2 substrates. To test this hypothesis, MCF-7 and MCF-7/MR cells were exposed to the established ABCG2 transport substrates MR [11] and topotecan [12]. Consistent with our previous results, MCF-7/MR cells were 96- and 38-fold resistant to these anticancer drugs, respectively, relative to parental cells. Moreover, this marked MDR level was mediated by ABCG2 as it was fully reversed by Ko143, a potent and specific ABCG2 transport inhibitor (Fig. 4A and C). Importantly, inhibition of the Akt-signaling pathway with LY294002 resulted in MDR reversal, similarly to the effect mediated by Ko143; specifically, the IC_{50} values of MCF-7/MR cells exposed to MR were 646 ± 15 μM, whereas exposure to MR in the presence of LY294002 resulted in a dramatically lower IC_{50} value of 9.0 ± 1.2 μM (i.e. 72-fold sensitization). Consistently, when exposed to topotecan, the IC_{50} value of MCF-7/MR cells was 38.0 ± 6.5 μM, whereas in the presence of LY294002 the IC_{50} value dropped to 5.3 ± 1.7 μM (7-fold sensitization). Moreover, the cytotoxic activity exerted by LY294002 (20 μM) and MR (30 μM) alone resulted in 90.3 ± 6.7 and 72.0 ± 5.0% cell survival, respectively. Remarkably, the combination of both agents at the same concentrations resulted in a remarkable synergistic effect yielding as little as 7.5 ± 5.6% cell survival (Fig. 4B). Similarly, exposure to topotecan (10 μM) resulted in 65.0 ± 9.7% cell survival, whereas upon combination with LY294002, cell survival dropped to 25.0 ± 14.0% (Fig. 4D). Thus, these findings establish that inhibition of the Akt-signaling pathway overcomes MDR that is mediated by ABCG2-rich EVs.

3.5. Treatment of MCF-7/MR cells with specific ABCG2 transport inhibitors results in cytoplasmic retention of ABCG2 and gradual elimination of EVs

During the course of the current study we noted that 24 h incubation with the established ABCG2 transport inhibitors FTC

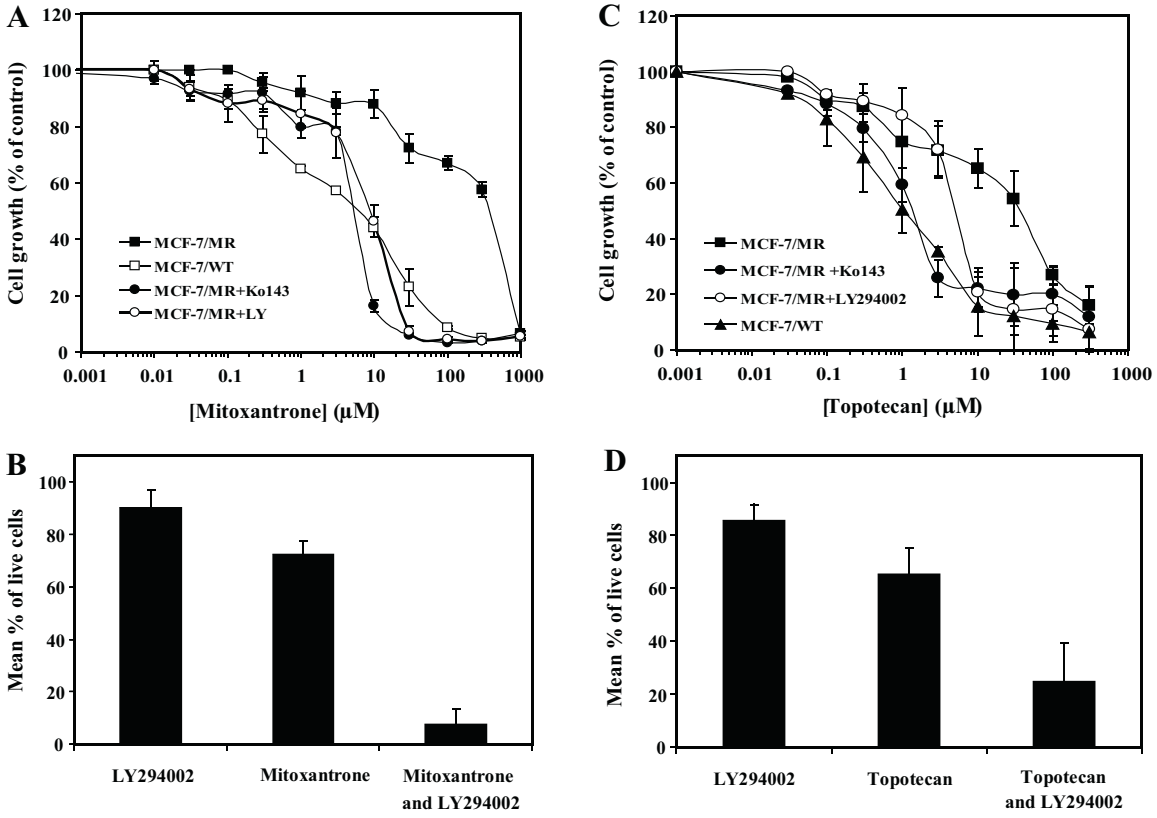

Fig. 4. Inhibition of the PI3K-Akt signaling pathway by LY294002 abolishes drug resistance to ABCG2-type cytotoxic drugs in MCF-7/MR cells. (A) MCF-7/MR cells were seeded in 96-well plates (400 cells/90 μl) and grown for 3 days to allow for EVs formation. Then, cells were pretreated with LY294002 (20 μM) for 90 min followed by 5 h co-exposure to increasing levels of MR. As a control, cells were co-incubated with the specific ABCG2 transport inhibitor Ko143 (0.7 μM) along with increasing concentrations of MR. At the end of the incubation period, cells were washed twice with fresh medium for 10 min each time, and incubated in fresh medium for additional 72 h prior to examination of cell viability. Cell viability was determined using the colorimetric XTT cell proliferation kit. Shown are the means of three independent experiments ± SD. A graphic illustration of the synergistic cytotoxic effect of LY294002 combined with MR in MCF-7/MR cells is depicted in (B). MCF-7/MR cells were incubated solely either with 20 μM LY294002 for 6.5 h or with 30 μM MR for 5 h; a different group of MCF-7/MR cells was pre-incubated with LY294002 for 90 min followed by co-incubation with MR for an additional 5 h, using the same drug concentrations. (C) MCF-7/MR cells were pretreated with LY294002 (20 μM) for 90 min following 72 h co-exposure to increasing concentrations of topotecan. As a control, cells were co-incubated with Ko143 (0.7 μM) along with increasing concentrations of topotecan. At the end of the incubation period, cells were analyzed as in (A). A graphic illustration of the synergistic cytotoxic effect of LY294002 combined with topotecan in MCF-7/MR cells is depicted in (D). MCF-7/MR cells were incubated solely either with 20 μM LY294002 for 6.5 h or with 10 μM topotecan for 72 h; a different group of MCF-7/MR cells was pre-incubated with LY294002 for 90 min followed by co-incubation with topotecan for an additional 72 h, using the same drug concentrations.

and Ko143 resulted in a marked decrease in the number of EVs. To corroborate this observation, we exposed MCF-7/MR cells to FTC (10 μM) or Ko143 (0.7 μM) for various times and used immunofluorescence microscopy to follow EVs as well as subcellular localization of vesicular markers including ABCG2 and ERM. We observed a time-dependent decrease in the number of EVs with both ABCG2 transport inhibitors (Fig. 5A). Specifically, drug-free control MCF-7/MR cells formed mature, ball-like shaped EVs where ABCG2 and ERM specifically co-localized at the EVs membrane (i.e. apical membrane; Fig. 5A, a–c). Under control conditions, no ABCG2 signal was observed at the cytoplasmic compartment or at the plasma membrane (i.e. basolateral membrane). However, following ABCG2 transport inhibition for 2–12 h, the number of EVs gradually decreased (Fig. 5A, d–o) with no residual EVs after 24 h (Fig. 5A, p–r). At the same time, the fluorescent ABCG2 signal appearing in the plasma membrane, sometimes forming crucifer-like structures, disclosing the original location of the disappearing EVs; there was also some cytoplasmic localization of ABCG2. This qualitative immunofluorescence microscopy analysis was evaluated quantitatively (Fig. 5B and C). Consistent with the results obtained with Akt-signaling inhibitors, ABCG2 transport inhibitors had no impact on ABCG2 protein levels (Fig. 5D). Moreover, the cytotoxic effect of Ko143 itself on MCF-7/MR cells and their parental MCF-7 cell line was also studied in order to rule out the possibility that cytoplasmic retention of ABCG2 is part of a general cellular response to apoptosis rather than a specific subcellular relocalization of ABCG2. Twenty-four hours of treatment with Ko143 followed by 48 h of incubation in a transport inhibitor-free medium resulted in Ko143 IC_{50} values of 22.4 ± 7.5 μM and 26.3 ± 9.4 μM in parental and MR-resistant cells, respectively. These results show that the concentration of Ko143 used in the ABCG2 transport inhibition studies (0.7 μM) was not cytotoxic.

4. Discussion

Recent studies suggested that the PI3K-Akt signaling pathway may contribute to the regulation of the subcellular localization of ABCG2; Mogi et al. [14] and Bleau et al. [15] showed that exposure of freshly isolated hematopoietic stem cells to the AKT inhibitor LY294002, resulted in translocation of ABCG2 from the plasma membrane to the cytoplasmic compartment. Consistently, Takada et al. [16], who examined ABCG2 localization in polarized LLC-PK-1 cells that were stably transfected with a human ABCG2 cDNA reported that Akt inhibition resulted in cytoplasmic internalization of ABCG2. We hence postulated that the PI3K-Akt signaling pathway may also play a role in the exclusive sorting of ABCG2 to the membrane of EVs in MCF-7/MR cells. ABCG2-rich EVs mimic lactating breast epithelium and serve as a reliable model for studying ABCG2-mediated MDR in breast cancer cells. Recently we

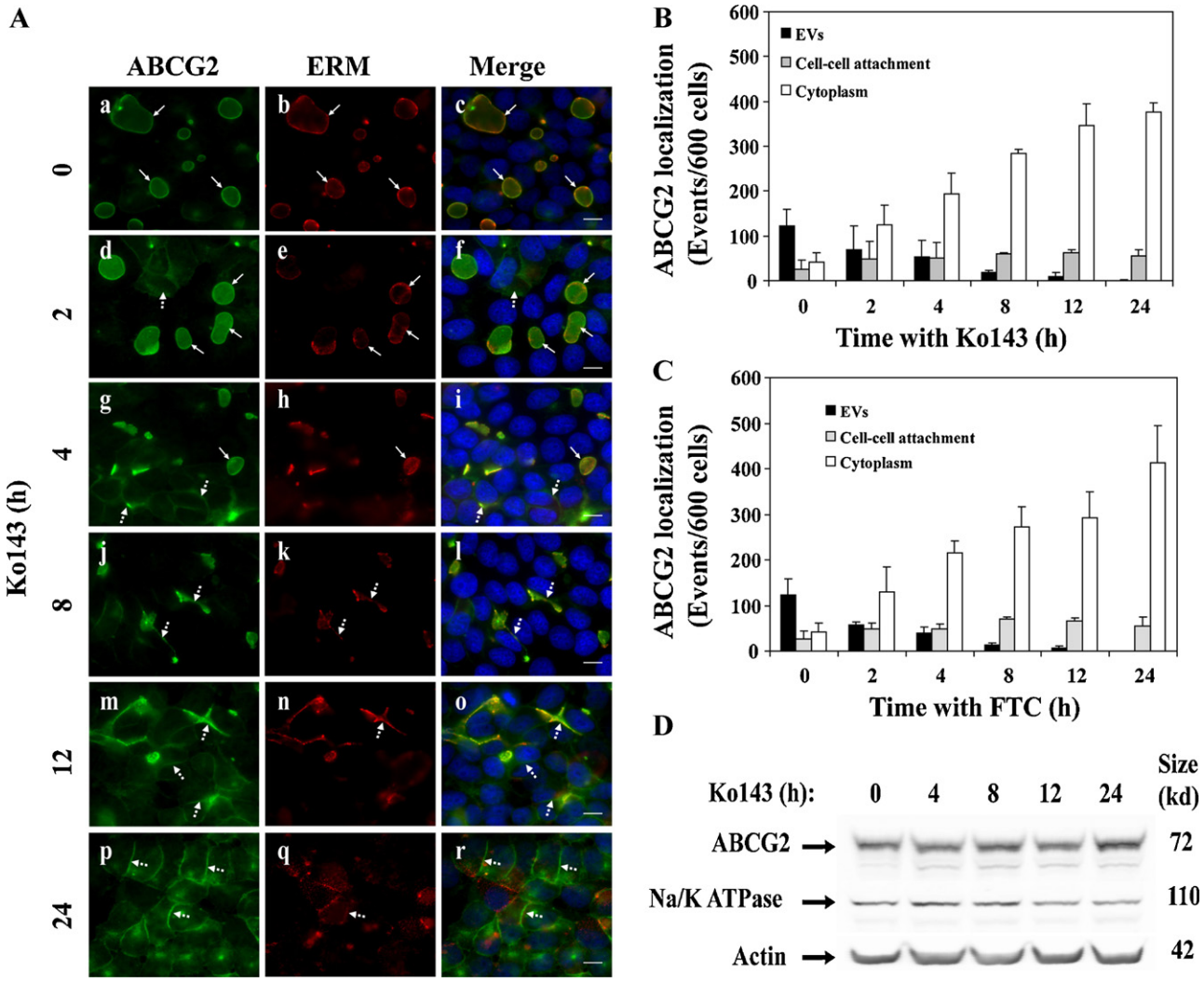

Fig. 5. Treatment of MCF-7/MR cells with ABCG2-specific transport inhibitors results in the cytoplasmic localization of ABCG2 and a dramatic decrease in the number of EVs. (A) MCF-7/MR cells were grown in 24-well plates on sterile glass coverslips for 7 days at 37 °C to allow for EVs formation. Then, cells were either untreated or treated with FTC (10 μM) or Ko143 (0.7 μM) for the indicated times. At the end of drug treatment, cells were washed thrice with PBS, fixed with 4% formaldehyde and co-reacted with anti-ABCG2 antibody (BXP-21) and with anti-ERM antibody. Nuclei were counterstained with DAPI. Random colonies were analyzed using Zeiss inverted Cell-Observer microscope at a magnification of 630×. *Continuous arrows* point at EVs displaying a co-localization of ABCG2 and ERM complex. *Dashed arrows* denote cells with plasma membrane and cytoplasmic localization of ABCG2 and ERM. A quantitative, graphic illustration of subcellular localization of ABCG2 following Ko143 (B) and FTC (C) treatment is depicted. MCF-7/MR cells were treated for the indicated times, stained and photographed as described in (A). Then, random fields were analyzed for ABCG2-rich EVs, plasma membrane localization or cytoplasmic localization of ABCG2. To generate these graphs, approximately 600 cells were examined for each time point. Graph represents three independent experiments ± SD. (D) MCF-7/MR cells were treated with Ko143 for the indicated times. Then, membrane proteins were extracted and equal amounts of protein (60 μg) were loaded for each time point, resolved on denaturing10% polyacrylamide gels and reacted with anti-ABCG2 antibody (BXP-53). Actual equal loading was verified using stripping and re-probing of the blot with anti-Na^+/K^+ ATPase and anti-actin antibodies.

found that EVs form not only in breast cancer cells but also in various human malignant tumor cells including gastric carcinoma N-87 cells [12] and non-small lung cancer A549/K1.5 cells [19]. Based on our present findings as well as on our previous results with ABCG2-rich EVs [11,12,19], we propose a composite model summarizing the impact of inhibition of the PI3K-Akt signaling pathway on the subcellular localization of ABCG2 as well as on the structure of EVs and their MDR function (Fig. 6A–C). We further expand this model to the marked impact of the ABCG2 transport inhibitors Ko143 and FTC on the targeting of ABCG2 to the membrane of EVs, in addition to their established activity as specific inhibitors of ABCG2-dependent drug transport (Fig. 6D and E). Specifically, activation of the PI3K-Akt pathway with EGF resulted in selective targeting of ABCG2 to the membrane of EVs (i.e. apical membrane). This unique localization of ABCG2 allowed for the efficient pumping and hence concentration of multiple cytotoxic agents of distinct structure and mode of action as well as non-toxic compounds including riboflavin [19] from the cytoplasm to the lumen of EVs. These cytotoxic agents included topotecan and MR ([12] and the current study), imidazoacridinones, methotrexate and Hoechst 33342 [12], hence representing various families of cytotoxic drugs. Inhibition of PI3K and its downstream cascade by LY294002 resulted in the cytoplasmic retention of ABCG2. Sorting of MDR efflux transporters of the ABC superfamily in polarized breast epithelial cells was poorly studied in the past, apparently due to the lack of suitable cell model systems. Towards this end, we have previously identified a structural and functional homology between EVs of MCF-7/MR breast cancer cells and bile canaliculi, on which extensive information is available regarding the trafficking and sorting of MDR efflux transporters [22]. These latter studies confirm that transporters of the ABC superfamily cycle between intracellular pools and the bile canalicular (apical) membrane before degradation [23,24]. Thus, lack of apical targeting of ABCG2 due to blockade of the Akt signaling axis markedly increases its cytoplasmic localization, thereby resulting in decreased drug accumulation within EVs and subsequent

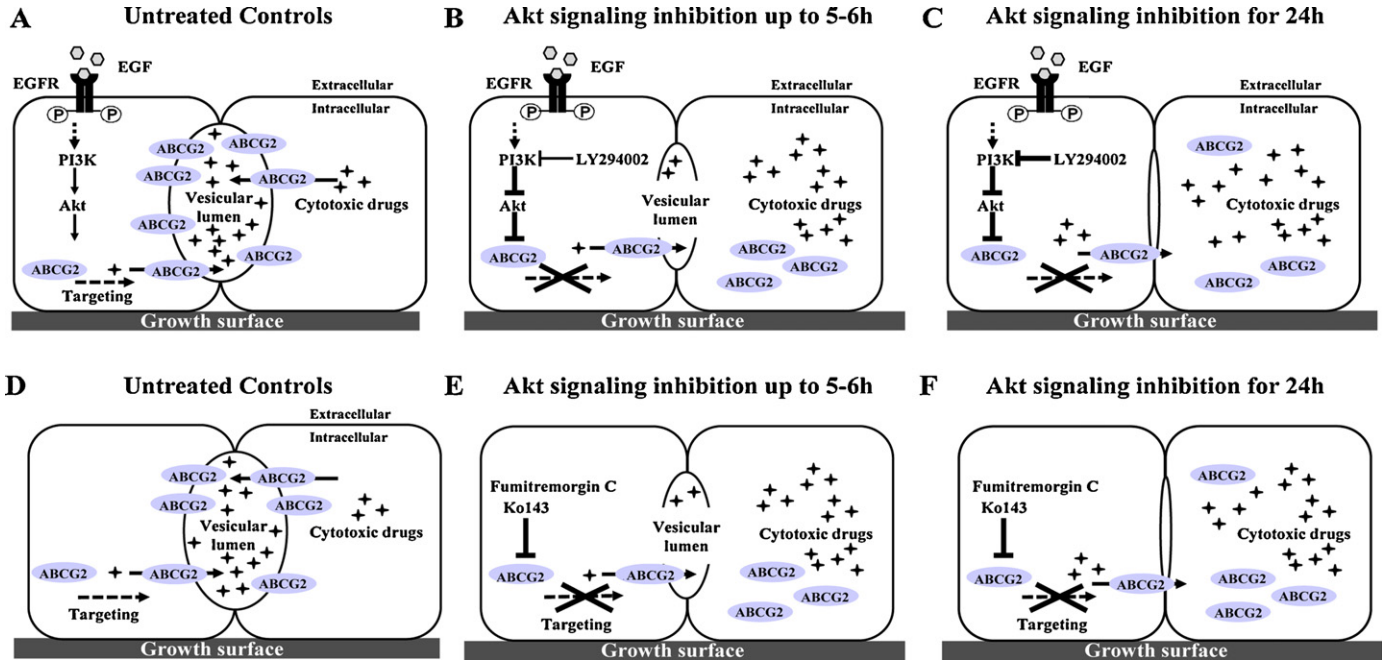

Fig. 6. A proposed model summarizing the impact of AKT-signaling inhibition or inhibition of ABCG2 drug transport on EVs structure and MDR function. (A and D) Upon EGF stimulation, the PI3K-Akt signaling is activated resulting in the targeting of ABCG2 to the EVs membrane, but not to the cell membrane facing the medium or neighbor cells. ABCG2 is overexpressed on the membrane of EVs where it highly concentrates multiple cytotoxic agents including topotecan, MR ([11] and current study), methotrexate, imidazoacridinones and Hoechst 33342 [11] as well as the B2-vitamin riboflavin [19]. (B) Following LY294002 treatment (90 min up to 5–6 h), ABCG2 targeting to the EVs membrane is blocked, thereby resulting in cytoplasmic retention of ABCG2 and subsequent gradual increase in the cytosolic fraction of drugs. Moreover, in the absence of apical targeting of ABCG2, EVs volume gradually decreased. (C) Following longer treatment with LY294002 (24 h), there was a dramatic fall in the volume and number of EVs, thereby resulting in the overcoming of MDR. A similar phenotype was observed when cells were treated with ABCG2-specific transport inhibitors FTC or Ko143 (E and F).

reversal of MDR. Moreover, such ABCG2 re-localization results in gradual elimination of EVs indicating that the PI3K-Akt signaling pathway is a key regulator of subcellular localization of ABCG2 and consequent biogenesis of EVs and their MDR function.

Recent studies identified a link between the PI3K-Akt signaling pathway and epithelial cell polarity. Specifically, Liu et al. [25] found that Akt and Rac1 act as downstream effectors of PI3K and function as control points of cellular proliferation and tissue polarity, respectively, in breast cancer cells. Moreover, Walid et al. [26] reported that the Akt signaling pathway plays a key role in epithelial cell remodeling as it regulates epithelial tubule formation in polarized MDCK cells. We have previously found that EVs are apically oriented in polarized MCF-7/MR cells [12]. Thus, it is reasonable to propose that the mechanism by which Akt signaling regulates apical trafficking of ABCG2 is possibly via regulation of cell polarity. Nevertheless, inhibition of ABCG2 by its specific transport inhibitors Ko143 and FTC, not only results in the expected inhibition of drug transport activity but also in the cytoplasmic retention of ABCG2, similarly to the effect observed when blocking apical targeting of ABCG2. These novel findings suggest that proper folding of ABCG2 and its targeting to the membrane of EVs are absolutely essential factors for the biogenesis of EVs and the MDR function.

Multiple drug resistance to chemotherapeutic agents remains a major cause of treatment failure in various human cancers. Aberrant activation of the PI3K-Akt pathway which is believed to be a major component contributing to the intrinsic insensitivity of cancer cells to chemotherapy, has been implicated in many cancers through several molecular mechanisms [27–29]. However, cumulative evidence indicated that in addition to intrinsic drug resistance, chemotherapy-induced resistance (i.e. acquired) may occur either by activation of the PI3K-Akt pathway and/or via the up-regulation of MDR efflux transporters of the ABC superfamily [30,31]. Thus, components of the PI3K-Akt pathway and the ABC superfamily of MDR transporters are key targets for chemotherapy. In this respect, it was previously recognized that a drug combination approach is required for successful chemotherapy. Indeed, several drug combination strategies have been studied; combining conventional chemotherapy with PI3K-Akt pathway inhibitors including LY294002 and wortmannin, Akt inhibitors perifosine and triciribine, and mTOR inhibitor rapamycin and its analogues have been investigated extensively in preclinical studies thereby demonstrating a synergistic efficacy *in vivo* [31,32]. Our current studies indicated that combining the Akt pathway inhibitor LY294002 with conventional chemotherapeutics including MR and topotecan, elicited a remarkable synergistic effect, thereby increasing the cytotoxic efficacy of the anticancer drugs treatment. Thus, these encouraging *in vitro* studies may be readily translatable to preclinical *in vivo* studies. An alternative approach combining pathway inhibitors with other targeted therapies includes inhibition of proximal pathway components such as receptor tyrosine kinases and oncogenes (her2/neu), combined with downstream inhibition of Akt or mTOR. This was suggested as an effective means of circumventing feedback activation that could occur with downstream inhibition alone. Small-molecule inhibitors of EGFR tyrosine kinase (TKIs) including gefitinib (ZD1839, Iressa) and erlotinib (OSI-774, Tarceva) which are FDA approved drugs ([33] and [34], respectively), have also shown promising clinical activities [35–37] when combined with conventional chemotherapeutics. However, acquired drug resistance to TKIs is associated with elevated expression of ABCG2, which in turn leads to efflux of TKIs from cancer cells [30,38–40]. Alternatively, dual inhibition of parallel signaling pathways prevents compensatory activation of redundant pro-survival pathways. Finally, inhibition of signaling pathways can be combined with several other types of targeted therapeutics including inhibition of histone deacetylase complexes (HDACs) or proteasome inhibitors [32]. In summary, based on the multifactorial nature of MDR and the frequent failure of clinical attempts to overcome MDR, we propose that in order to enhance treatment efficacy towards the ultimate goal of overcoming MDR, rationally

designed, specific synergistic combinations of chemotherapeutic drugs are highly required. Thus, we specifically propose here to target both key signaling pathways such as the PI3K-Akt signaling axis in combination with transport inhibitors or cytotoxic substrates of the ABC superfamily of transporters including ABCG2, which are established key mediators of MDR.

Acknowledgments

We thank Dr. G.L. Scheffer and Prof. R. Scheper, Department of Pathology, VU University Medical Center, Amsterdam, The Netherlands for the generous gift of BXP-21 and BXP-53 antibodies and Prof. S.J. Karlish, Department of Biological Chemistry, The Weizmann Institute of Science, Rehovot, Israel for the anti-KETTY antibody. We extend our gratitude to Dr. K. Smid and Prof. G.J. Peters, Department of Medical Oncology, VU University Medical Center, Amsterdam, The Netherlands for their kind gift of topotecan. We kindly acknowledge the Life Sciences and Engineering Infrastructure Unit (Technion, Israel) for their expert technical assistance with the various microscopy experiments.

Appendix A. Supplementary data

Supplementary data associated with this article can be found, in the online version, at doi:10.1016/j.bcp.2012.01.033.

References

[1] Dillon RL, White DE, Muller WJ. The phosphatidyl inositol 3-kinase signaling network: implications for human breast cancer. Oncogene 2007;26:1338–45.
[2] Garcia-Echeverria C, Sellers WR. Drug discovery approaches targeting the PI3K/Akt pathway in cancer. Oncogene 2008;27:5511–26.
[3] Wickenden JA, Watson CJ. Key signalling nodes in mammary gland development and cancer. Signalling downstream of PI3 kinase in mammary epithelium: a play in 3 Akts. Breast Cancer Res 2010;12:202.
[4] Martelli AM, Evangelisti C, Chiarini F, McCubrey JA. The phosphatidylinositol 3-kinase/Akt/mTOR signaling network as a therapeutic target in acute myelogenous leukemia patients. Oncotarget 2010;1:89–103.
[5] Borst P, Elferink RO. Mammalian ABC transporters in health and disease. Annu Rev Biochem 2002;71:537–92.
[6] Haimeur A, Conseil G, Deeley RG, Cole SP. The MRP-related and BCRP/ABCG2 multidrug resistance proteins: biology, substrate specificity and regulation. Curr Drug Metab 2004;5:21–53.
[7] Sarkadi B, Ozvegy-Laczka C, Nemet K, Varadi A. ABCG2—a transporter for all seasons. FEBS Lett 2004;567:116–20.
[8] Gottesman MM, Fojo T, Bates SE. Multidrug resistance in cancer: role of ATP-dependent transporters. Nat Rev Cancer 2002;2:48–58.
[9] Szakacs G, Paterson JK, Ludwig JA, Booth-Genthe C, Gottesman MM. Targeting multidrug resistance in cancer. Nat Rev Drug Discov 2006;5:219–34.
[10] Assaraf YG. Molecular basis of antifolate resistance. Cancer Metastasis Rev 2007;26:153–81.
[11] Ifergan I, Scheffer GL, Assaraf YG. Novel extracellular vesicles mediate an ABCG2-dependent anticancer drug sequestration and resistance. Cancer Res 2005;65:10952–58.
[12] Goler-Baron V, Structure Assaraf YG. Function of ABCG2-rich extracellular vesicles mediating multidrug resistance. PLoS One 2011;6:e16007.
[13] Allen JD, van Loevezijn A, Lakhai JM, van der Valk M, van Tellingen O, Reid G, et al. Potent and specific inhibition of the breast cancer resistance protein multidrug transporter *in vitro* and in mouse intestine by a novel analogue of fumitremorgin C. Mol Cancer Ther 2002;1:417–25.
[14] Mogi M, Yang J, Lambert JF, Colvin GA, Shiojima I, Skurk C, et al. Akt signaling regulates side population cell phenotype via BCRP1 translocation. J Biol Chem 2003;278:39068–75.
[15] Bleau AM, Hambardzumyan D, Ozawa T, Fomchenko EI, Huse JT, Brennan CW, et al. PTEN/PI3K/Akt pathway regulates the side population phenotype and ABCG2 activity in glioma tumor stem-like cells. Cell Stem Cell 2009;4:226–35.
[16] Takada T, Suzuki H, Gotoh Y, Sugiyama Y. Regulation of the cell surface expression of human BCRP/ABCG2 by the phosphorylation state of Akt in polarized cells. Drug Metab Dispos 2005;33:905–9.
[17] Nakanishi T, Shiozawa K, Hassel BA, Ross DD. Complex interaction of BCRP/ABCG2 and imatinib in BCR-ABL-expressing cells: BCRP-mediated resistance to imatinib is attenuated by imatinib-induced reduction of BCRP expression. Blood 2006;108:678–84.
[18] Taylor CW, Dalton WS, Parrish PR, Gleason MC, Bellamy WT, Thompson FH, et al. Different mechanisms of decreased drug accumulation in doxorubicin and mitoxantrone resistant variants of the MCF7 human breast cancer cell line. Br J Cancer 1991;63:923–9.
[19] Ifergan I, Goler-Baron V, Assaraf YG. Riboflavin concentration within ABCG2-rich extracellular vesicles is a novel marker for multidrug resistance in malignant cells. Biochem Biophys Res Commun 2009;380:5–10.
[20] Ifergan I, Shafran A, Jansen G, Hooijberg JH, Scheffer GL, Assaraf YG. Folate deprivation results in the loss of breast cancer resistance protein (BCRP/ABCG2) expression. A role for BCRP in cellular folate homeostasis. J Biol Chem 2004;279:25527–34.
[21] Ifergan I, Jansen G, Assaraf YG. Cytoplasmic confinement of breast cancer resistance protein (BCRP/ABCG2) as a novel mechanism of adaptation to short-term folate deprivation. Mol Pharmacol 2005;67:1349–59.
[22] Wakabayashi Y, Kipp H, Arias IM. Transporters on demand: intracellular reservoirs and cycling of bile canalicular ABC transporters. J Biol Chem 2006;281:27669–73.
[23] Gatmaitan ZC, Nies AT, Arias IM. Regulation and translocation of ATP-dependent apical membrane proteins in rat liver. Am J Physiol 1997;272:G1041–49.
[24] Kipp H, Pichetshote N, Arias IM. Transporters on demand: intrahepatic pools of canalicular ATP binding cassette transporters in rat liver. J Biol Chem 2001;276:7218–24.
[25] Xu J, Liu Y, Yang Y, Bates S, Zhang JT. Characterization of oligomeric human half-ABC transporter ATP-binding cassette G2. J Biol Chem 2004;279:19781–89.
[26] Walid S, Eisen R, Ratcliffe DR, Dai K, Hussain MM, Ojakian GK. The PI 3-kinase and mTOR signaling pathways are important modulators of epithelial tubule formation. J Cell Physiol 2008;216:469–79.
[27] Jiang BH, Liu LZ. PI3K/PTEN signaling in tumorigenesis and angiogenesis. Biochim Biophys Acta 2008;1784:150–8.
[28] Nicholson KM, Anderson NG. The protein kinase B/Akt signalling pathway in human malignancy. Cell Signal 2002;14:381–95.
[29] Song G, Ouyang G, Bao S. The activation of Akt/PKB signaling pathway and cell survival. J Cell Mol Med 2005;9:59–71.
[30] Chen YJ, Huang WC, Wei YL, Hsu SC, Yuan P, Lin HY, et al. Elevated BCRP/ABCG2 expression confers acquired resistance to gefitinib in wild-type EGFR-expressing cells. PLoS One 2011;6:e21428.
[31] Huang WC, Hung MC. Induction of Akt activity by chemotherapy confers acquired resistance. J Formos Med Assoc 2009;108:180–94.
[32] LoPiccolo J, Blumenthal GM, Bernstein WB, Dennis PA. Targeting the PI3K/Akt/mTOR pathway: effective combinations and clinical considerations. Drug Resist Updat 2008;11:32–50.
[33] Cohen MH, Williams GA, Sridhara R, Chen G, Pazdur R. FDA drug approval summary: gefitinib (ZD1839) (Iressa) tablets. Oncologist 2003;8:303–6.
[34] Cohen MH, Johnson JR, Chen YF, Sridhara R, Pazdur R. FDA drug approval summary: erlotinib (Tarceva) tablets. Oncologist 2005;10:461–6.
[35] Fukuoka M, Yano S, Giaccone G, Tamura T, Nakagawa K, Douillard JY, et al. Multi-institutional randomized phase II trial of gefitinib for previously treated patients with advanced non-small-cell lung cancer (The IDEAL 1 Trial) [corrected]. J Clin Oncol 2003;21:2237–46.
[36] Kris MG, Natale RB, Herbst RS, Lynch Jr TJ, Prager D, Belani CP, et al. Efficacy of gefitinib, an inhibitor of the epidermal growth factor receptor tyrosine kinase, in symptomatic patients with non-small cell lung cancer: a randomized trial. J Am Med Assoc 2003;290:2149–58.
[37] Perez-Soler R, Chachoua A, Hammond LA, Rowinsky EK, Huberman M, Karp D, et al. Determinants of tumor response and survival with erlotinib in patients with non-small-cell lung cancer. J Clin Oncol 2004;22:3238–47.
[38] Nakamura Y, Oka M, Soda H, Shiozawa K, Yoshikawa M, Itoh A, et al. Gefitinib (Iressa, ZD1839), an epidermal growth factor receptor tyrosine kinase inhibitor, reverses breast cancer resistance protein/ABCG2-mediated drug resistance. Cancer Res 2005;65:1541–6.
[39] Shi Z, Parmar S, Peng XX, Shen T, Robey RW, Bates SE, et al. The epidermal growth factor tyrosine kinase inhibitor AG1478 and erlotinib reverse ABCG2-mediated drug resistance. Oncol Rep 2009;21:483–9.
[40] Shi Z, Peng XX, Kim IW, Shukla S, Si QS, Robey RW, et al. Erlotinib (Tarceva, OSI-774) antagonizes ATP-binding cassette subfamily B member 1 and ATP-binding cassette subfamily G member 2-mediated drug resistance. Cancer Res 2007;67:11012–20.